

Probability of Error for Optimal Codes in a Reconfigurable Intelligent Surface Aided URLLC System

Likun Sui, Zihuai Lin, *Senior Member, IEEE*,

Abstract—The lower bound on the decoding error probability for the optimal code given a signal-to-noise ratio and a code rate are investigated in this letter for the reconfigurable intelligent surface (RIS) communication system over a Rician fading channel at the short blocklength regime, which is the key characteristic of ultra-reliable low-latency communications (URLLC) to meet the need for strict adherence to quality of service (QoS) requirements. Sphere packing technique is used to derive our main results. The Wald sequential t-test lemma and the Gaussian-Chebyshev quadrature are the main tools to obtain the closed-form expression for the lower bound. Numerical results are provided to validate our results and demonstrate the tightness of our results compared to the Polyanskiy-Poor-Verdu (PPV) bound.

Index Terms—Reconfigurable intelligent surfaces, ultra-reliable and low-latency communications, Lower bound, decoding error probability, sphere packing

I. INTRODUCTION

NOWADAYS, industrial communications have differed significantly from conventional wireless communications as they necessitate deterministic communication with stringent quality of service requirements. These requirements include ultra-reliable and low-latency communications (URLLC), achieved by exchanging a small amount of data such as control commands or measurement data. For URLLC, it is crucial to maintain a maximum transmission latency of one millisecond, while ensuring the packet error probability falls within the range of 10^{-6} to 10^{-9} [1], [2]. To surmount the aforementioned obstacle, the reconfigurable intelligent surface (RIS) has emerged as a promising solution that has piqued significant research interest from both academia and industry [3]–[8]. To avoid the disconnection due to blockages by the obstacles, the RIS is regarded as a promising solution, which the RIS stands apart from conventional relay technologies by transforming the harsh propagation environment into a favorable one, due to its distinctive properties. These properties enhance the signal quality at the receiver side without requiring any additional power consumption and increase the diversity gain [27]. In contrast to existing relay technologies, the RIS can transform an unfavorable propagation environment into a favorable one due to its unique characteristics, which can improve signal quality at the receiver side without requiring more power. In addition to higher data rates, low latency is an essential factor that we must prioritize. Applications of the

Internet of Things (IoT) [9]–[12] and the fifth Generation (5G) communication system [13]–[19] need to balance between low latency and high accuracy. An RIS is a panel, typically square or circular, composed of numerous reflecting elements. These elements induce independent phase shifts on the impinging electromagnetic (EM) waves. By meticulously designing the phase shifts of each element, the reflected EM waves can be constructively added to the direct signal from the base station (BS), but at most time the direct signal is blocked by an obstacle, increasing the signal power at the intended user and improving the system’s signal-to-noise (SNR) performance.

As a result, the performance analysis for the RIS system at the short blocklength regime is much needed. Most of the existing contributions on the performance analysis in the short blocklength focus on the fundamental channel model, i.e., the additive white Gaussian noise (AWGN) channel. The authors in [20] identified Shannon’s lower bound, specifically the sphere packing bound, as the superior choice for the AWGN channel, setting it as a benchmark for comparison against other bounds, such as the Gallager bound, Feinstein bound, and their own Polyanskiy-Poor-Verdu (PPV) bound. In [21], the authors demonstrated that the sphere packing bound provides an optimal lower bound for low-rate codes up to a specific blocklength, which can extend to several thousands. Additionally, the majority of existing works on RIS concentrate on the optimization of the active beamforming at the BS and the phase shift matrix at the RIS for different channel state information (CSI). In [22], the authors derived the average decoding error probability using the PPV bound with a Gaussian input for RIS-aided communications.

Contributions: 1) This letter investigates the sphere packing bounds for evaluating the performance of an RIS-aided wireless system over a Rician fading channel at a short blocklength regime. 2) Using Wald sequential t-test lemma and the Gaussian-Chebyshev quadrature, we obtain a closed-form expression for the bound. 3) The approximation of the angle in the sphere packing technique used to determine the code rate in [23] and [21] will have a margin of error at a short blocklength regime, which we overcome by deriving the expression to calculate the exact value of the angle. 4) The results are validated through some numerical and Monte-Carlo simulation results and we set the PPV bound [20] as a reference.

Likun Sui, and Zihuai Lin are with the *School of Electrical and Information Engineering, The University of Sydney*, Sydney, NSW 2006, Australia (e-mail: likun.sui@sydney.edu.au; zihuai.lin@sydney.edu.au).

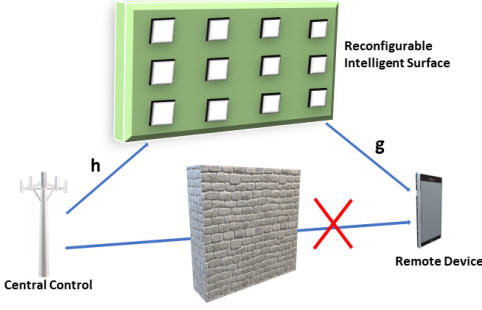


Fig. 1: System model for the RIS-aided wireless system

II. SYSTEM MODEL

As shown in Fig. 1, we consider an RIS-aided transmission system with the direct link blocked by an obstacle, i.e., a wall or building, between the single-element transmit and receive antennas. In this letter, we focus on enhancing the overall system performance by employing a rectangular RIS consisting of N_{ris} elements. We assume that all the RIS elements are ideal which means that each of them can independently influence the phase, which can be flexibly adjusted, and the reflection angle of the impinging wave.

The signal vector at the receive antenna is given by

$$y(i) = \sqrt{P_r} A(i) s(i) + w(i), \quad i = 1, \dots, n, \quad (1)$$

where n and i denote the blocklength and its i -th entry and $w(i)$ is the equivalent baseband AWGN with a zero mean and variance N_0 , i.e., $w(i) \sim \mathcal{CN}(0, N_0)$, and $A(i)$ is the end-to-end channel coefficient, P_r is the average power at the receiver, which can be obtained from the Friis path-loss model [24] as

$$P_r = \frac{P G_t G_r \lambda^2}{16\pi^2 (d_1 + d_2)^2}, \quad (2)$$

where P is signal power at the transmitter, and λ is the wavelength in meters, and G_t and G_r are the transmitter and receiver antenna gains. d_1 and d_2 denote the distance between the transmitter and the RIS, the RIS and the receiver, respectively. We assume that the binary phase shift keying (BPSK) modulation is adopted in the air interface. The transmitted signal $s(i) \in \mathcal{A}$, $i = 1, \dots, n$, where $\mathcal{A} = \{-1, +1\}$.

We denote the baseband equivalent channels between the transmitter and the m -th reflecting element of the RIS by $\mathbf{h}_m = [h_m(1), \dots, h_m(n)]$, $\forall m = 1, \dots, N_{ris}$ with $h_m(i) = |h_m(i)| e^{j\phi_m(i)}$, where $|h_m(i)|$ and $\phi_m(i)$ represent the amplitude and phase of the channel coefficient $h_m(i)$, respectively. The reflecting channels between the m -th reflecting element and the receiver are $\mathbf{g}_m = [g_m(1), \dots, g_m(n)]$ with $g_m(i) = |g_m(i)| e^{j\varphi_m(i)}$, where $|g_m(i)|$ and $\varphi_m(i)$ represent the amplitude and phase of the channel coefficient $g_m(i)$, respectively. The channels are assumed to be independent and identically distributed (i.i.d), and their envelopes follow the Rician distribution, i.e., we have $|h_m(i)| \sim \text{Rician}(\zeta_1, \eta_1)$, where the shape parameter of the Rician fading $K_1 = \eta_1^2 / (2\zeta_1^2)$ denotes the ratio of the power contributions by a line-of-sight path to the remaining multipaths, and the scale parameter of the Rician fading $\Omega = 2\zeta_1^2 + \eta_1^2$ is the total power received in all paths. We assume that the probability density

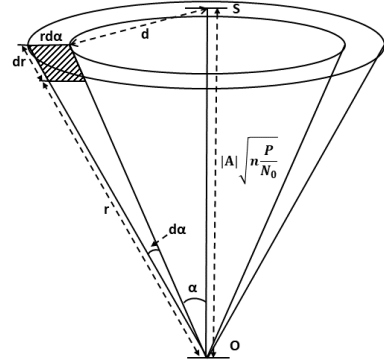


Fig. 2: Plane of cone of angle α

function (PDF) of $|g_m(i)|$ is also Rician distributed, i.e., $|g_m(i)| \sim \text{Rician}(\zeta_2, \eta_2)$. Then, $A(i)$ of our RIS-aided system can be expressed as

$$A(i) = \sum_{m=1}^{N_{ris}} \eta_m(i) h_m(i) g_m(i), \quad (3)$$

where $\eta_m(i)$ denotes the reflecting coefficient of the m -th reflecting element with $\eta_m(i) = |\eta_m(i)| e^{j\theta_m(i)}$, where $|\eta_m(i)|$ represents the reflecting gain and $\theta_m(i)$ is the phase shift configured by the m -th reflecting element. Without loss of generality, we assume the reflecting gain $|\eta_m(i)| = 1$. In addition, we assume that the phases of the channels $h_m(i)$ and $g_m(i)$ are perfectly known to the transmitter, and that the RIS can choose the optimal phase shifting, i.e., $\theta_m(i) = -(\phi_m(i) + \varphi_m(i))$. Hence, (3) can be re-written as

$$A(i) = \sum_{m=1}^{N_{ris}} |h_m(i)| \cdot |g_m(i)| \quad (4)$$

In Fig. 2, we assume that O is the origin of an n -dimensional sphere and S is a signal point which situates on the surface of the n dimensional sphere. α denotes the angle of the cone intersected by the two outer lines and the angle $\alpha + d\alpha$ is the slightly larger angle which represents a larger cone. The radius of the outer cone is $r + dr$, and that of the inner cone is r . Therefore, the two sides of the ring-shaped plane are $r d\alpha$ and dr , respectively. d presents the distance between the signal point S and the above ring. We consider that there is a channel code with the number of codewords M . For notation simplicity, in the following, we use A instead of $A(i)$, the code can place its M points arbitrarily on the surface of the n -dimensional sphere whose radius is $|A| \sqrt{n \frac{P}{N_0}}$.

III. PERFORMANCE ANALYSIS

A. The lower Bound

Theorem 1. For any $\alpha_1 < \frac{\pi}{2}$, given the channel coefficient A , the conditional probability of error $P_{e, opt}^L(n, R|A)$ for the optimal code with the length n , and code rate R can be lower-bounded by

$$P_{e, opt}^L(n, R|A) \geq \Phi(\alpha, n, A), \quad (5)$$

where $\Phi(\alpha, n, A)$ denotes the probability of a signal point S in the n -dimensional sphere, which has the $|A| \sqrt{n \frac{P}{N_0}}$

distance between the origin point O , being moved outside the cone whose angle is α . And $\Lambda(\alpha, n)$ denotes the $(n-1)$ -dimensional area of the cap, which is cut out by the cone on the $(n-1)$ -dimensional unit sphere. And α_1 is the angle which can even cut the sphere into M parts, equivalently $M\Lambda(\alpha_1, n) = \Lambda(\pi, n)$. Then by taking the expectation over the channel coefficient A , the lower bound of the error probability $P_{e, opt}^L(n, R)$ for the optimal code with the length n , and code rate R can be finally obtained as

$$P_{e, opt}^L(n, R) \geq \mathbb{E}_A[\Phi(\alpha, n, A)]. \quad (6)$$

where the parameter α_1 is determined by solving the equation

$$2^{nR}\Lambda(\alpha_1, n) = \Lambda(\pi, n). \quad (7)$$

The proof of Theorem 1 can be found in [23] [21].

According to Theorem 1, at first, we need to calculate $\Lambda(\alpha_1, n)$. The surface of an n -dimensional sphere with an r radius can be given as $S_n(r) = n\pi^{n/2}r^{n-1}/\Gamma(\frac{n+2}{2})$. According to the cosine law and the fact of the $(n-1)$ -dimensional unit sphere, we obtain that the radius of the cap is $\sin \alpha$. Thus, we get

$$\Lambda(\alpha_1, n) = \frac{(n-1)\pi^{\frac{n-1}{2}}}{\Gamma(\frac{n+1}{2})} \int_0^{\alpha_1} \sin^{n-2} \alpha d\alpha. \quad (8)$$

From (8), we can easily get

$$\Lambda(\pi, n) = S_n(1) = \frac{n\pi^{n/2}}{\Gamma(\frac{n+2}{2})}. \quad (9)$$

In order to decrease the margin of error at the short blocklength regime and get the exact expression for $\Lambda(\alpha, n)$, we need to calculate $\int_0^\alpha (\sin \alpha)^{n-2} d\alpha$ which is defined by the recursive relationship for all $n > 3$

$$\begin{aligned} \Pi(\alpha, n) &= \int_0^\alpha (\sin \alpha)^{n-2} d\alpha \\ &= -\sin^{n-3} \alpha \cos \alpha + (n-3) \int_0^\alpha \cos^2 \alpha \sin^{n-4} \alpha d\alpha \\ &= -\frac{\sin^{n-3} \alpha \cos \alpha}{n-2} + \frac{n-3}{n-2} \Pi(\alpha, n-2) \end{aligned}$$

and by the initial conditions $\Pi(\alpha, 2) \triangleq \alpha$ and $\Pi(\alpha, 3) \triangleq -\cos \alpha$.

For numerical accuracy purposes, we use this recursive relationship to compute the value of $\Pi(\alpha, n)$, and times the coefficient, then we have $\Lambda(\alpha, n) = \Pi(\alpha, n)(n-1)\pi^{\frac{n-1}{2}}/\Gamma(\frac{n+1}{2})$. When n is even, we have

$$\begin{aligned} \Lambda(\alpha, n) &= \frac{(n-1)\pi^{\frac{n-1}{2}}}{\Gamma(\frac{n+1}{2})} \left(\frac{(n-3)!!}{(n-2)!!} \alpha - \frac{\sin^{n-3} \alpha \cos \alpha}{n-2} \right. \\ &\quad \left. - \sum_{i=0}^{\frac{n}{2}-1} \sin^{n-5-2i} \alpha \cos \alpha \frac{\prod_{j=\frac{n}{2}-i}^{\frac{n}{2}} (2j-3)}{\prod_{k=\frac{n}{2}-(i+1)}^{\frac{n}{2}} (2k-2)} \right) \quad (10) \end{aligned}$$

and when n is odd, we have

$$\begin{aligned} \Lambda(\alpha, n) &= \frac{(1-n)\pi^{\frac{n-1}{2}}}{\Gamma(\frac{n+1}{2})} \left(\frac{(n-3)!!}{(n-2)!!} \cos \alpha + \frac{\sin^{n-3} \alpha \cos \alpha}{n-2} \right. \\ &\quad \left. + \sum_{i=0}^{\frac{n}{2}-1} \sin^{n-5-2i} \alpha \cos \alpha \frac{\prod_{j=\frac{n}{2}-i}^{\frac{n}{2}} (2j-3)}{\prod_{k=\frac{n}{2}-(i+1)}^{\frac{n}{2}} (2k-2)} \right), \quad (11) \end{aligned}$$

where $(\cdot)!!$ denotes the double factorial. Then we need to calculate $\Phi(\alpha, n)$, which corresponds to the probability of signal point S being carried outside the cone by the noise. The noise, of which the mean value and variance are zero and one, respectively, is generated by an n -dimensional Gaussian distribution function

$$f(d) = \frac{1}{(2\pi)^{n/2}} e^{-d^2/2}. \quad (12)$$

Based on the cosine law from Fig. 2, we have the expression for d which is shown below

$$d^2 = r^2 + A^2 n \frac{P}{N_0} - 2rA \sqrt{n \frac{P}{N_0}} \cos \alpha. \quad (13)$$

The differential volume of the ring-shaped region equals the shaded area, which is $rdrd\alpha$ times the surface of an $(n-1)$ -dimensional sphere whose radius is $r \sin \theta$

$$\begin{aligned} dV &= r dr d\alpha S_{n-1}(r \sin \alpha) \\ &= r dr d\alpha \frac{(n-1)\pi^{\frac{n-1}{2}} (r \sin \alpha)^{n-2}}{\Gamma(\frac{n+1}{2})}. \quad (14) \end{aligned}$$

We multiply the PDF in (12) and the differential volume in (14) and then substitute d from (13). Therefore, we can get the expression for $\Phi(\alpha)$,

$$\begin{aligned} \Phi(\alpha, n, A) &= \frac{(n-1) \exp(-\frac{1}{2} A^2 n \frac{P}{N_0})}{2^{n/2} \pi^{1/2} \Gamma(\frac{n+1}{2})} \int_{\alpha_1}^{\pi/2} \sin^{n-2} \alpha \\ &\quad \int_0^\infty r^{n-1} \exp(-\frac{1}{2} r^2 + rA \sqrt{n \frac{P}{N_0}} \cos \alpha) dr d\alpha \\ &\quad + Q(A \sqrt{n \frac{P}{N_0}}), \quad (15) \end{aligned}$$

where $Q(\cdot)$ is the Q function, $Q(x) = \frac{1}{\sqrt{2\pi}} \int_x^\infty \exp(-\frac{1}{2} t^2) dt$.

In order to simplify (15) and reduce its complexity, our objective is to derive the closed form of $\Phi(\alpha, n, A)$ by eliminating integrals with respect to r and α . Initially, we can achieve this by leveraging the Wald sequential t -test lemma in [25] to eliminate the integral with respect to r which is shown as follows

$$\begin{aligned} &\int_0^\infty r^{n-1} \exp(-\frac{1}{2} r^2 + rA \sqrt{n \frac{P}{N_0}} \cos \alpha) dr \\ &\approx \sqrt{2\pi} \Delta(\alpha, n) \left(\frac{\nabla(\alpha, n)}{e} \right)^{n-1} \exp\left(\frac{1}{2} \nabla^2(\alpha, n, A)\right), \quad (16) \end{aligned}$$

where

$$\begin{aligned} \nabla(\alpha, n, A) &\triangleq A \nabla(\alpha, n) = \\ &\sqrt{n} A \left(\frac{1}{2} \sqrt{\frac{P}{N_0}} \cos \alpha + \sqrt{\frac{P \cos^2 \alpha}{4N_0} + \frac{n-1}{n(k_2 - k_1^2)}} \right) \end{aligned}$$

and

$$\Delta(\alpha, n) \triangleq \frac{1}{2} \left(\left(1 + \frac{k_2 - k_1^2}{4} \left(\sqrt{A^2 \cos^2 \alpha \frac{P}{N_0} + \frac{4}{k_2 - k_1^2}} \right. \right. \right. \\ \left. \left. \left. - A \cos \alpha \sqrt{\frac{P}{N_0}} \right)^2 \right)^{-1/2} + \sqrt{\frac{\nabla^2(\alpha, n)}{\nabla^2(\alpha, n) + \frac{n-1}{k_2 - k_1^2}}} \right),$$

where $k_1 = \mathbb{E}[A] = \frac{1}{4}\pi N_{ris} L_{1/2}(-K_1) L_{1/2}(-K_2)$ and $k_2 = \text{Var}[A] = N_{ris}((1 + K_1)(1 + K_2) - \frac{1}{16}\pi^2 L_{1/2}^2(-K_1) L_{1/2}^2(-K_2))$ with $L_p(\cdot)$ denotes the Laguerre polynomial. Then, we have

$$\Phi(\alpha, n, A) \approx Q\left(A\sqrt{n\frac{P}{N_0}}\right) + \frac{(n-1)}{e^{n-1}2^{(n-1)/2}\Gamma(\frac{n+1}{2})} \\ \int_{\alpha_1}^{\pi/2} \frac{\Delta(\alpha, n)}{\nabla(\alpha, n, A) \sin^2 \alpha} \exp\left(-n\left(\frac{1}{2}\frac{A^2 P}{N_0} - \frac{1}{2n}\nabla^2(\alpha, n, A) \right. \right. \\ \left. \left. - \log(\nabla(\alpha, n, A) \sin \alpha)\right)\right) d\alpha. \quad (17)$$

Then, to eliminate the integral with respect to α , we utilize the Gaussian-Chebyshev quadrature. according to [26], the Gaussian-Chebyshev quadrature has been widely used in the state-of-the-art works since it approximates the integrals with limited terms to reduce the computational complexity while obtaining a good accuracy. Then, we have the closed-form expression for $\Phi(\alpha, n, A)$ as follows

$$\Phi(\alpha, n, A) \approx Q\left(A\sqrt{n\frac{P}{N_0}}\right) + \frac{1}{e^{n-1}2^{(n-1)/2}\Gamma(\frac{n+1}{2})} \\ \sum_{i=1}^K \frac{(\pi/2 - \alpha_1)w_i\sqrt{1 - \phi_i}\Delta(s_i, n)}{2\nabla(s_i, n, A) \sin^2 s_i} \exp\left(-n\left(\frac{1}{2}\frac{A^2 P}{N_0} \right. \right. \\ \left. \left. - \frac{1}{2n}\nabla^2(s_i, n, A) - \log(\nabla(s_i, n, A) \sin s_i)\right)\right), \quad (18)$$

where

$$s_i = \frac{\pi/2 - \alpha_1}{2}\psi_i + \frac{\pi/2 + \alpha_1}{2} \quad (19)$$

with $\psi_i = \cos(\frac{2i-1}{2K}\pi)$ and $w_i = \frac{\pi}{K}$. Moreover, we need to get the probability density of the channel coefficient A to calculate the expectation over A . The PDF of A in (4) can be statistically evaluated as [27]

$$f_A(x) = \frac{x^a}{b^{a+1}\Gamma(a+1)} \exp\left(-\frac{x}{b}\right), \quad (20)$$

where

$$a = \frac{k_1^2}{k_2} - 1 \quad \text{and} \quad b = \frac{k_2}{k_1}. \quad (21)$$

Finally, applying the following lemma, we combine (20) and (18) together to obtain the closed-form expression for the lower bound denoted as $P_{e, opt}^L(n, R)$ in (23), where $X(\alpha, n) = nP/(2N_0) - \nabla^2(\alpha, n)/2$, and s_i is given in (19), and a, b are given in (21) with $P = \frac{16\pi^2(d_1+d_2)^2 P_r}{G_t G_r \lambda^2}$.

Lemma 1. For the integral from negative infinity to infinity

$$\int_{-\infty}^{\infty} A^a \exp\left(-cA^2 - \frac{A}{b}\right) dA,$$

the closed-form expression is shown below

$$\frac{1}{2}c^{-\frac{a+2}{2}} \left(\sqrt{c}\Gamma\left(\frac{1+a}{2}\right) {}_1F_1\left(\frac{1+a}{2}, \frac{1}{2}, \frac{1}{4b^2c}\right) \right. \\ \left. - \frac{1}{b}\Gamma\left(1 + \frac{a}{2}\right) {}_1F_1\left(1 + \frac{a}{2}, \frac{3}{2}, \frac{1}{4b^2c}\right) \right), \quad (22)$$

where ${}_1F_1(\cdot, \cdot, \cdot)$ denotes Kummer confluent hypergeometric function.

Compared with the approximation of α_1 in [23] [21] which is tightly suitable when R and n grow relatively large. To compute the exact value of α_1 in (7) at a short blocklength regime, in the case of an even n , we use (10) divided by (9) to obtain the exact value of α_1 . Otherwise, we use (11) divided by (9) to calculate α_1 .

B. Asymptotic Formula

At large enough blocklength, there exist some asymptotic formula to give a very good approximation of the bound and to allow all the computations in the logarithmic domain. We investigate the asymptotic formula of our derived result over the RIS system. At first, we define $G(\alpha, A) \triangleq AG(\alpha) = \frac{A}{2}\left(\sqrt{\frac{P}{N_0}}\cos\alpha + \sqrt{\frac{P}{N_0}\cos^2\alpha + \frac{4}{k_2 - k_1^2}}\right)$. Then, the asymptotic formula for the lower bound is shown below.

$$P_{e, opt, asymptotic}^L \geq \mathbb{E}_A \left[\frac{\sqrt{n-1}}{6n(A\sqrt{\frac{P}{N_0}} + 1)} \right. \\ \left. \exp\left\{ -\frac{(A\sqrt{\frac{P}{N_0}} + 1)^2 + 3}{2} - n\left(\frac{A^2 P}{2N_0} - \frac{1}{2}G(\alpha_1, A)A \right. \right. \right. \\ \left. \left. \left. \sqrt{\frac{P}{N_0}}\cos\alpha_1 - \log(G(\alpha_1, A)\sin\alpha_1)\right)\right\} \right]. \quad (24)$$

Moreover, we have the PDF of the channel coefficient A in (20). Thus, after applying Lemma 1, we have the closed-form expression of the asymptotic formula for the lower bound which is shown below

$$P_{e, opt, asymptotic}^L \geq \frac{\sqrt{n-1}G^n(\alpha_1)\sin^n\alpha_1}{12e^2n\sqrt{\frac{P}{N_0}}\xi^{a+n}\Gamma(a+n)} \\ X_2^{-\frac{a+n+1}{2}}(\alpha_1, n) \left(\sqrt{X_2(\alpha_1, n)}\Gamma\left(\frac{a+n}{2}\right) \right. \\ {}_1F_1\left(\frac{a+n}{2}, \frac{1}{2}, \frac{1}{4\xi^2 X_2(\alpha_1, n)}\right) - \frac{1}{\xi}\Gamma\left(\frac{a+n+1}{2}\right) \\ \left. {}_1F_1\left(\frac{a+n+1}{2}, \frac{3}{2}, \frac{1}{4\xi^2 X_2(\alpha_1, n)}\right) \right), \quad (25)$$

where $X_2(\alpha_1, n) = \frac{(n+1)P}{2N_0} - \frac{nG(\alpha_1)\cos\alpha_1}{2}\sqrt{\frac{P}{N_0}}$ and $\xi = \frac{b}{1+b\sqrt{\frac{P}{N_0}}}$ with $P = \frac{16\pi^2(d_1+d_2)^2 P_r}{G_t G_r \lambda^2}$.

IV. COMPARISON AND ANALYSIS

In this section, we compare the lower bound for different blocklength and numbers of the RIS elements. Fig. 3 illustrates the comparison between the lower bound on the MLD decoding error probability for the codes with the code length

$$P_{e, opt}^L(n, R) = \frac{1}{e^{n-1} 2^{(n+1)/2} b^{a+n} \Gamma(a+n) \Gamma(\frac{n+1}{2})} \sum_{i=1}^K \frac{(\pi/2 - \alpha_1 w_i \sqrt{1 - \phi_i}) \Delta(s_i, n)}{\nabla^{-n+1}(s_i, n) \sin^{-n+2}(s_i)} X^{-\frac{a+n+1}{2}}(s_i, n) (\sqrt{X(s_i, n)} \Gamma(\frac{a+n}{2}) {}_1F_1(\frac{a+n}{2}, \frac{1}{2}, \frac{1}{4b^2 X(s_i, n)}) - \frac{1}{b} \Gamma(\frac{a+n+1}{2}) {}_1F_1(\frac{a+n+1}{2}, \frac{1}{2}, \frac{1}{4b^2 X(s_i, n)})) \quad (23)$$

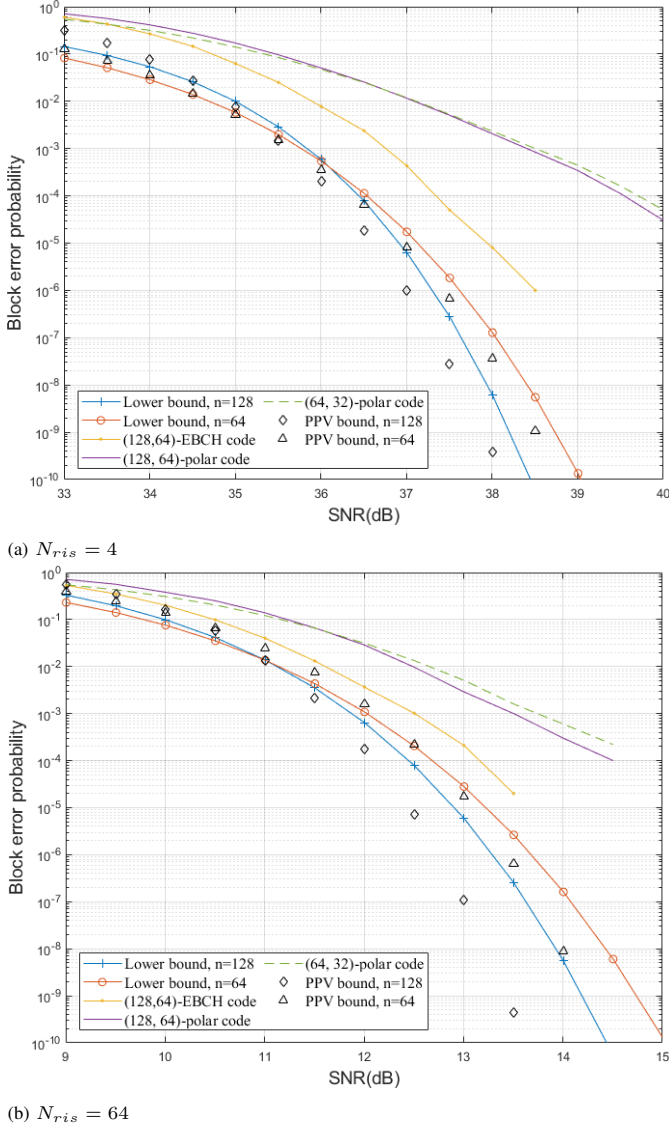


Fig. 3: A comparison between the lower bound on the MLD decoding error probability for the codes of code length $n = 64$ bits and $n = 128$ bits with the same code rate $R = 0.5$ bits per channel use over the perfect Rician fading channel in Section III for different number of RIS elements.

$n = 128$ bits and $n = 64$ bits and with the same code rate $R = 0.5$ bits per channel use over the perfect Rician fading channel where the shape parameters K_1 and K_2 are chosen as 1 and 0.5 in Section III for different numbers of RIS elements 4 and 64, respectively. We define the transmit SNR as $\frac{P}{N_0}$ in decibels (dB) and set $P_r = 0$ dB, the wavelength $\lambda = 0.125m$ (the operating frequency $f_c = 2.4$ GHz), $G_t = G_r = 8$ (9.03 dBi) and $d_1 = d_2 = 10m$. We utilize the Polar code with the SCL decoder and the EBCH code with the OSD decoder to validate our bounds. All the simulations are averaged by 10^6 Monte Carlo realizations. We set the PPV

bound in [20] as a reference. From Fig. 3(a), we observe that at the low SNR regime, the performance of the code with the short blocklength, i.e., $n = 64$, is slightly better than the one with the long blocklength, i.e., $n = 128$. When we increase the SNR, the long code will finally outperform the short code. The SNR's value of the intersection on the lower bounds is approximately 36 dB. It indicates that the short code is preferred when the targeted SNR is less than 36 dB. Otherwise, we can choose the long code to accomplish better transmission. In Fig. 3(a), in terms of the code length of 128 bits, for a decoding error probability of 10^{-2} , the gap between the lower bound and the EBCH code is 0.8 dB. When the decoding error probability level is low i.e., 10^{-4} , the gap increases to 1.0 dB.

Fig. 3(b) shows, as N_{ris} increase from 4 to 64, the comparison between the performances of the lower bound of the different code length with the same code rate. When it comes to $n = 128$ bits, for the decoding error probability of 10^{-2} , the gap between its lower bound and the polar code is 0.7 dB. It validates our derived result with different number of RIS elements. Furthermore, the SNR's value of the intersection on the lower bounds is approximately 11 dB. In this work, we only simulated EBCH and polar codes, in the future work, we will also try different codes, such as rateless codes [28]–[31] and convolutional codes [32]–[37].

V. CONCLUSION

This letter investigated the lower bound of the decoding error probability for the optimal code of the specific length, SNR and code rate for the RIS assisted URLLC communication system over a Rician fading channel at a short blocklength regime. The sphere packing technique is mainly used to derive our derived bound with the closed-form expression. Numerical and Monte-Carlo simulation results of EBCH and polar codes validate the derived results and demonstrate that the tightness of our results is better than the PPV bound at the high SNR regime.

REFERENCES

- [1] Z. Pang, M. Luvisotto, and D. Dzung, "Wireless high-performance communications: The challenges and opportunities of a new target," in *IEEE Ind. Electron. Mag.*, vol. 11, no. 3, pp. 20–25, Sep. 2017.
- [2] M. Shirvanimoghadam, M. Mohamadi, R. Abbas, A. Minja, C. Yue, B. Matuz, G. Han, Z. Lin, Y. Li, S. Johnson, and B. Vucetic "Short Blocklength Codes for Ultra-Reliable Low-Latency Communications", *IEEE Communications Magazine*, Volume: 57, Issue: 2, February 2019.
- [3] X. Wang, Z. Lin, F. Lin, and L. Hanzo, "Joint hybrid 3d beamforming relying on sensor-based training for reconfigurable intelligent surface aided terahertz-based multi-user massive mimo systems," in *IEEE Sens. J.*, pp. 1–1, 2022.
- [4] Z. Chu, P. Xiao, D. Mi, W. Hao, Z. Lin, Q. Chen, and R. Tafazolli, "Wireless powered intelligent radio environment with non-linear energy harvesting," in *IEEE Internet Things J.*, pp. 1–1, 2022.

- [5] Y. Hu, P. Wang, Z. Lin, and M. Ding, "Performance analysis of reconfigurable intelligent surface assisted wireless system with low-density parity-check code," in *IEEE Commun. Lett.*, vol. 25, no. 9, pp. 2879–2883, 2021.
- [6] L. Sui, Z. Lin, "Analytical Bounds for the Optimal Code over the Reconfigurable Intelligent Surface at a Short Blocklength", *IEEE Wireless Communications Letters*, Early Access, Jun. 2023. doi: 10.1109/LWC.2023.3283528.
- [7] L. Sui, Z. Lin, P. Xiao, and B. Vucetic, "Performance Analysis for Reconfigurable Intelligent Surface Assisted MIMO Systems", *IEEE Transaction on Wireless Communications*, Early Access, May. 2023. doi:10.1109/TWC.2023.3277887.
- [8] L. Sui, Z. Lin, P. Xiao, B. Vucetic and H. Poor, "Performance Analysis of Multiple-Antenna Ambient Backscatter Systems at Finite Blocklengths", *IEEE Internet of Things Journal*, Early Access, Apr. 2023. doi:10.1109/JIOT.2023.3267130.
- [9] J. Leng, Z. Lin and P. Wang, "An implementation of an internet of things system for smart hospitals", 2020 IEEE/ACM Fifth International Conference on Internet-of-Things Design and Implementation (IoTDI), 254–255, 2020.
- [10] D. Zhai, H. Chen, Z. Lin, Y. Li and B. Vucetic, "Accumulate Then Transmit: Multi-user Scheduling in Full-Duplex Wireless-Powered IoT Systems", *IEEE Internet of Things Journal*, Volume: 5, Issue: 4, Aug. 2018.
- [11] J. Wang, B. Li, G. Wang, Z. Lin, H. Wang, and G. Chen, Optimal Power Splitting for MIMO SWIPT Relaying Systems with Direct Link in IoT Networks, *Physical Communication*, Volume 43, December 2020.
- [12] Z. Lin and W. Xiang, "Wireless Sensing and Networking for the Internet of Things", MDPI books, ISBN 978-3-0365-7448-6 (hardback); ISBN 978-3-0365-7449-3.
- [13] M. Ding, D. López-Pérez, Y. Chen, G. Mao, Z. Lin and A. Y. Zomaya, "Ultra-Dense Networks: A Holistic Analysis of Multi-Piece Path Loss, Antenna Heights, Finite Users and BS Idle Modes," in *IEEE Transactions on Mobile Computing*, vol. 20, no. 4, pp. 1702-1713, 1 April 2021, doi: 10.1109/TMC.2019.2960223.
- [14] J. Yang, M. Ding, G. Mao and Z. Lin, "Interference Management in In-Band D2D Underlaid Cellular Networks," in *IEEE Transactions on Cognitive Communications and Networking*, vol. 5, no. 4, pp. 873-885, Dec. 2019, doi: 10.1109/TCCN.2019.2927568.
- [15] J. Yang, M. Ding, G. Mao, Z. Lin and X. Ge, "Analysis of Underlaid D2D-Enhanced Cellular Networks: Interference Management and Proportional Fair Scheduler," in *IEEE Access*, vol. 7, pp. 35755-35768, 2019, doi: 10.1109/ACCESS.2019.2904966.
- [16] J. Yang, M. Ding, G. Mao, Z. Lin, "Optimal Base Station Antenna Downtilt in Downlink Cellular Networks", *IEEE Transactions on Wireless Communications* On page(s): 1-13 Print ISSN: 1536-1276 Online ISSN: 1558-2248 Digital Object Identifier: 10.1109/TWC.2019.2897296.
- [17] Z. Lin, B. Vucetic, J. Mao, "Ergodic capacity of LTE downlink multiuser MIMO systems", 2008 IEEE International Conference on Communications, 3345-3349.
- [18] Y. Chen, M. Ding, D. Lopez-Perez, X. Yao, Z. Lin, and G. Mao, "On the theoretical analysis of network-wide massive mimo performance and pilot contamination," *IEEE Transactions on Wireless Communications*, vol. 21, no. 2, pp. 1077–1091, 2022.
- [19] G. Mao, Z. Lin, X. Ge, Y. Yang, "Towards a simple relationship to estimate the capacity of static and mobile wireless networks", *IEEE transactions on wireless communications* 12 (8), 2014, 3883-3895
- [20] Y. Polyanskiy, H. V. Poor and S. Verdú, "Channel Coding Rate in the Finite Blocklength Regime," in *IEEE Trans. Inf. Theory*, vol. 56, no. 5, pp. 2307-2359, May 2010.
- [21] A. Valembois and M. P. C. Fossorier, "Sphere-packing bounds revisited for moderate block lengths," in *IEEE Trans. Inf. Theory*, vol. 50, no. 12, pp. 2998-3014, Dec. 2004.
- [22] H. Ren, K. Wang and C. Pan, "Intelligent Reflecting Surface-Aided URLLC in a Factory Automation Scenario," in *IEEE Trans. Commun.*, vol. 70, no. 1, pp. 707-723, Jan. 2022.
- [23] C. E. Shannon, "Probability of error for optimal codes in a Gaussian channel," in *Bell Syst. Tech. J.*, vol. 38, no. 3, pp. 611-656, May 1959.
- [24] W. Tang et al., "Path Loss Modeling and Measurements for Reconfigurable Intelligent Surfaces in the Millimeter-Wave Frequency Band," in *IEEE Trans. Commun.*, vol. 70, no. 9, pp. 6259-6276, Sept. 2022
- [25] William Kruskal, "The monotonicity of the ratio of two noncentral t density functions," in *Ann. Math. Stat.*, Vol. 25, pp. 162-165, 1954.
- [26] Y. Liu, Z. Ding, M. ElKashlan, and H. V. Poor, "Cooperative nonorthogonal multiple access with simultaneous wireless information and power transfer," in *IEEE J. Sel. Areas Commun.*, vol. 34, no. 4, pp. 938–953, Apr. 2016.
- [27] A. -A. A. Boulogeorgos and A. Alexiou, "Performance Analysis of Reconfigurable Intelligent Surface-Assisted Wireless Systems and Comparison With Relaying," in *IEEE Access*, vol. 8, pp. 94463-94483, 2020.
- [28] J. Yue, Z. Lin, B. Vucetic, G. Mao, T. Aulin, "Performance analysis of distributed raptor codes in wireless sensor networks", *IEEE Transactions on Communications* 61 (10), 2013, 4357-4368
- [29] P. Wang, G. Mao, Z. Lin, M. Ding, W. Liang, X. Ge, Z. Lin, "Performance analysis of raptor codes under maximum likelihood decoding", *IEEE Transactions on Communications* 64 (3), 2016, 906-917
- [30] K. Pang, Z. Lin, Y. Li, B. Vucetic, "Joint network-channel code design for real wireless relay networks", the 6th International Symposium on Turbo Codes & Iterative Information, 2010, 429-433.
- [31] J. Yue, Z. Lin and B. Vucetic, "Distributed Fountain Codes With Adaptive Unequal Error Protection in Wireless Relay Networks," in *IEEE Transactions on Wireless Communications*, vol. 13, no. 8, pp. 4220-4231, Aug. 2014, doi: 10.1109/TWC.2014.2314632.
- [32] Z. Lin, A. Svensson, "New rate-compatible repetition convolutional codes", *IEEE Transactions on Information Theory* 46 (7), 2651-2659
- [33] Z. Lin and T. Aulin, "Joint Source and Channel Coding using Punctured Ring Convolutional Coded CPM", *IEEE Transactions on Communications*, Vol. 56, No. 5, May, 2007, pp. 712-723.
- [34] Z. Lin and T. Aulin, "On Combined Ring Convolutional Coded Quantization and CPM for Joint Source and Channel Coding", *Transactions on Emerging Telecommunications Technologies*, Special Issue on 'New Directions in Information Theory', Vol.19, No.4. June 2008, pp. 443-453.
- [35] Z. Lin and T. Aulin, "Joint Source-Channel Coding using Combined TCQ/CPM: Iterative Decoding", *IEEE Transactions on Communications*, VOL.53, NO. 12, Dec. 2005, pp. 1991-1995.
- [36] Z. Lin and B. Vucetic, "Performance Analysis on Ring Convolutional Coded CPM", *IEEE Transactions on Wireless Communications*, Vol. 8, No. 9, Sept. 2009, pp. 4848-4854.
- [37] Z. Lin and T. Aulin, "On Joint Source and Channel Coding using trellis coded CPM: Analytical Bounds on the Channel Distortion", *IEEE Transactions on Information Theory*, Vol. 53, No. 13, Sept. 2007. pp. 3081-3094.